

Axion Masses as an Inevitable Consequence of Supersymmetry Breaking

Gayatri Ghosh^{1,*}

¹*Department of Physics, Institute for Advanced Fundamental Studies, India*

(Dated: January 8, 2026)

We investigate a supersymmetric framework in which soft supersymmetry-breaking effects provide the dominant origin of Peccei–Quinn (PQ) symmetry breaking and axion mass generation. In the supersymmetric limit the theory possesses an exact PQ symmetry and a massless axion, while the inclusion of soft terms proportional to the gravitino mass induces spontaneous PQ breaking, stabilizes the saxion direction, and generates a mass for the axion. As a consequence, the axion, saxion, and axino masses are all controlled by the supersymmetry-breaking scale, leading to a correlated and predictive spectrum of axion-like states.

The presence of explicit soft PQ-breaking terms raises the question of vacuum alignment and CP violation. We show that although the axion mass does not originate from QCD instantons, the induced strong CP phase is parametrically suppressed by the hierarchy between the QCD-induced and soft-induced axion masses. As a result, the explicit breaking does not generate an observable CP-violating vacuum angle across the parameter space of interest.

We analyze the phenomenological implications of this scenario, including axion lifetimes, axion–photon couplings, and laboratory, astrophysical, and cosmological constraints. Direct confrontations with beam-dump and collider searches, together with Big Bang nucleosynthesis bounds, demonstrate that a substantial region of parameter space remains viable and testable. The framework thus provides a self-consistent and phenomenologically rich realization of axion-like particles whose masses arise predominantly from soft supersymmetry breaking.

1. INTRODUCTION

The axion was originally proposed as a solution to the strong CP problem through the Peccei–Quinn mechanism [1, 2] and has since emerged as a well-motivated extension of the Standard Model, with implications for particle physics, astrophysics, and cosmology. Depending on the ultraviolet completion and symmetry-breaking structure, axions and axion-like particles may span a wide range of masses and couplings[3–6]. Recent years have seen significant progress in axion and axion-like particle searches, both from helioscope experiments such as CAST and from upcoming facilities like IAXO [8, 9]. Next-generation helioscopes are expected to significantly extend the sensitivity to axion–photon couplings over a wide mass range [11–13]. In the MeV–GeV mass range, laboratory probes including beam-dump and flavour experiments provide leading sensitivity, notably from NA64 and Belle. Despite these advances, the origin of axion masses in theories with approximate global symmetries remains an open theoretical question, particularly in the presence of supersymmetry breaking and quantum-gravity effects. In this work we show that axion masses arise inevitably from soft supersymmetry-breaking terms, leading to predictive correlations between the axion mass, couplings, and lifetime. We construct a minimal supersymmetric framework in which the axion mass vanishes in the supersymmetric limit and is generated solely by soft breaking effects. We analyze the resulting cosmological and experimental constraints and

identify statistically preferred regions of parameter space that can be tested by current and future experiments.

The Peccei–Quinn (PQ) symmetry provides one of the most compelling solutions to the strong CP problem of quantum chromodynamics (QCD) by promoting the CP-violating vacuum angle to a dynamical field, the axion. In its original formulation, the PQ symmetry is a global symmetry that is exact at the classical level and is broken spontaneously at a scale f_a , giving rise to a pseudo-Goldstone boson [7, 10] whose mass is generated dominantly by non-perturbative QCD effects. The resulting axion mass is inversely proportional to the PQ-breaking scale and is therefore naturally small. The exact origin of the PQ symmetry breaking scale and its possible connection to other fundamental scales in nature, however, remain open questions.

A theoretically well-motivated extension of the Standard Model (SM) is provided by supersymmetry [14, 15], which stabilizes the electroweak scale against large radiative corrections and improves the unification of gauge couplings. In its minimal realization, supersymmetry is implemented through the minimal supersymmetric standard model (MSSM). The phenomenological viability of this framework requires supersymmetry to be broken at a scale not far above the electroweak scale. In supergravity-based theories, this breaking is parameterized by soft supersymmetry-breaking terms whose overall magnitude is set by the gravitino mass $m_{3/2}$. The MSSM mass spectrum is thus controlled by the μ parameter and the soft supersymmetry-breaking scale, both of which are expected to lie close to the TeV scale.

The axion sector and the supersymmetry-breaking sector are, in general, treated as independent extensions of the SM. In conventional supersymmetric axion models,

* corresponding.author@example.com

such as the KSVZ or DFSZ frameworks [16, 17], the PQ symmetry breaking scale f_a is introduced as an external input, typically many orders of magnitude above the electroweak and supersymmetry-breaking scales. In these constructions, the axion mass is generated predominantly by QCD dynamics, while supersymmetry-breaking effects mainly determine the masses of the axion superpartners, namely the saxion and the axino [18, 19]. As a result, there is no intrinsic connection between the PQ-breaking scale and the supersymmetry-breaking scale.

In this work, we point out an alternative and conceptually appealing scenario in which the soft supersymmetry-breaking terms induced by supergravity not only break supersymmetry but also provide the sole origin of Peccei–Quinn symmetry breaking and axion mass generation. In the supersymmetric limit, the theory possesses an exact global PQ symmetry and a massless axion. Once supersymmetry is broken, the soft terms proportional to $m_{3/2}$ trigger spontaneous PQ symmetry breaking, stabilize the scalar potential of the PQ sector, and generate an axion mass entirely from soft supersymmetry-breaking effects. In this way, the PQ-breaking scale and the axion mass become directly linked to the gravitino mass.

The amalgamation of the PQ-breaking scale with the supersymmetry-breaking scale provides a compelling reason to expect axion-related physics at comparatively low energy scales if supersymmetry is invoked to address the gauge hierarchy problem or to achieve precision gauge coupling unification. In the framework proposed here, the axion, saxion, and axino masses are all controlled by the same underlying supersymmetry-breaking dynamics, leading to a predictive axion supermultiplet spectrum. While the axion mass generated in this way generally exceeds the conventional QCD axion mass, we show that viable regions of parameter space exist in which the axion behaves as a consistent axion-like particle without reintroducing the strong CP problem.

It is worth noting that connections between axion physics and supersymmetry breaking have been explored in a variety of contexts in the literature. In several models, the PQ symmetry is broken independently of supersymmetry breaking, with the axion remaining essentially massless until QCD effects are taken into account. In other approaches, the stabilization of the saxion field and the generation of axino masses rely on supersymmetry-breaking effects, while the axion mass itself remains dominated by QCD dynamics. In contrast, the framework presented here establishes a direct and inherent link between supersymmetry breaking and the origin of the axion mass, thereby offering a more unified and predictive setup for the axion sector. In this work we investigate a qualitatively different realization of axion physics, in which the axion mass originates solely from soft supersymmetry-breaking effects. In the supersymmetric limit, the theory possesses an exact Peccei–Quinn symmetry and a strictly massless axion. The inclusion of soft supersymmetry-breaking terms, induced for instance by supergravity, simultaneously triggers sponta-

neous PQ symmetry breaking and generates a finite axion mass. As a result, the axion mass vanishes continuously in the limit of unbroken supersymmetry, establishing a direct and controlled link between the axion sector and the supersymmetry-breaking scale. This mechanism sharply contrasts with conventional QCD axion models and generic axion-like particle scenarios, where explicit PQ-breaking effects are typically present already at the supersymmetric level. The framework therefore provides a predictive setting in which the properties of the axion supermultiplet—including the axion, saxion, and axino—are governed by the soft-breaking parameters, leading to distinctive phenomenological and cosmological implications. This connection between axion physics and supersymmetry breaking offers a new perspective on PQ symmetry breaking and motivates a systematic exploration of axion phenomenology beyond the standard QCD axion paradigm. Unlike generic axion-like particle constructions, the axion mass in this framework is not an independent soft parameter but an unavoidable consequence of the same supersymmetry-breaking dynamics that generate the MSSM soft spectrum. It is worth emphasizing how the present framework differs from earlier supersymmetric axion constructions. While soft supersymmetry-breaking effects have long been known to play an important role in stabilizing the saxion and axino sectors, existing models typically introduce the axion mass either through QCD effects or via explicit PQ-breaking operators whose size is independent of supersymmetry breaking. In contrast, the defining feature of the present setup is that the axion mass vanishes identically in the supersymmetric limit and is generated entirely by soft supersymmetry-breaking terms. As a result, the axion mass is not a free parameter but a calculable consequence of the supersymmetry-breaking sector.

Throughout this work we consider a minimal supersymmetric effective field theory describing the Peccei–Quinn (PQ) sector, coupled to supergravity. The model contains a single gauge-singlet chiral superfield \hat{S} carrying a non-zero PQ charge and neutral under the Standard Model gauge group. In the supersymmetric limit, the theory is defined by a scale-invariant, renormalizable superpotential

$$W = \frac{\kappa}{3} \hat{S}^3, \quad (1)$$

which respects an exact global $U(1)_{\text{PQ}}$ symmetry and gives rise to a massless axion. Supersymmetry breaking is assumed to be mediated by supergravity, inducing soft terms of order the gravitino mass $m_{3/2}$. Among these, a holomorphic bilinear soft term $B_S S^2$ explicitly breaks the PQ symmetry and constitutes the sole source of axion mass generation in the low-energy theory. No explicit PQ-violating operators are present at the supersymmetric level. Quantum-gravity-induced PQ violation is assumed to be sufficiently suppressed, for instance due to an accidental PQ symmetry enforced by a discrete gauge remnant or a broken gauged symmetry in the ultraviolet.

let completion. The analysis is performed at the level of the effective field theory, without specifying a unique ultraviolet completion, and focuses on the generic and unavoidable consequences of soft supersymmetry breaking for axion physics.

This definition makes explicit that our results are model-independent within the class of supersymmetric effective theories satisfying the above assumptions.

The remainder of this paper is organized as follows. In section 2, we present the basic mechanism by which soft supersymmetry-breaking terms induce spontaneous PQ symmetry breaking and generate an axion mass. Section 3 contains a detailed analysis of the axion supermultiplet spectrum, including the axion, saxion, and axino masses. In section 4, we study the axion couplings to gauge fields and fermions and discuss the associated phenomenological constraints. Section 5 is devoted to astrophysical and cosmological implications of the framework, while section 6 addresses possible experimental signatures and discovery prospects. Our conclusions are summarized in section 7.

2. PECCEI–QUINN SYMMETRY BREAKING FROM SOFT SUPERSYMMETRY BREAKING

In this section, we present the basic theoretical framework in which the breaking of the Peccei–Quinn (PQ) symmetry and the generation of the axion mass originate entirely from soft supersymmetry-breaking effects. In the supersymmetric limit, the low-energy theory exhibits an accidental Peccei–Quinn symmetry, which is preserved by the renormalizable interactions of the effective theory but may be violated by higher-dimensional operators suppressed by the Planck scale. A comment is in order concerning the status of the Peccei–Quinn symmetry in the present framework. While quantum gravity is expected to violate exact global symmetries, the PQ symmetry here should be understood as an accidental low-energy symmetry, arising from a more fundamental ultraviolet completion. In particular, the structure of the superpotential and Kähler potential can be enforced by a discrete gauge symmetry, such as a \mathbb{Z}_N symmetry, or by the remnant of a gauged $U(1)$ symmetry broken at a high scale. In such constructions, potentially dangerous Planck-suppressed PQ-violating operators are either forbidden or appear only at sufficiently high dimension. As a consequence, the leading PQ-violating operators induced by quantum gravity take the schematic form

$$\Delta\mathcal{L}_{\text{grav}} \sim \frac{S^n}{M_{\text{Pl}}^{n-4}} + \text{h.c.}, \quad n \geq N, \quad (2)$$

where N is determined by the underlying discrete symmetry. For sufficiently large N , the induced contribution to the axion potential is parametrically suppressed relative to the soft supersymmetry-breaking effects discussed in this work. In the present scenario, the PQ-breaking scale is tied to the supersymmetry-breaking

scale, $f_a \sim m_{3/2}/\kappa$, and is therefore significantly below the Planck scale. Nevertheless, provided that the leading PQ-violating operators arise at dimension $n \gtrsim 8$, their contribution to the axion mass remains subdominant compared to the soft-induced mass,

$$m_{a,\text{grav}}^2 \ll m_{a,\text{soft}}^2, \quad (3)$$

ensuring that the axion dynamics are controlled by supersymmetry breaking rather than by gravitational effects. To place the present construction in context, we stress that many supersymmetric axion models rely on either QCD instanton effects or explicit superpotential terms to generate the axion mass, with soft terms entering only as subleading corrections. In such scenarios, the axion mass scale is largely decoupled from the supersymmetry-breaking scale. By contrast, in the framework considered here, the axion remains exactly massless in the supersymmetric limit, and the leading contribution to its mass arises solely from soft supersymmetry-breaking operators. This leads to a qualitatively different parametric structure in which the axion, saxion, and axino masses are all controlled by the same underlying scale. We emphasize that the novelty of the present work does not lie in the existence of soft contributions to axion-sector masses per se, but in the fact that supersymmetry breaking provides the sole and unavoidable origin of the axion mass itself.

2.1. Supersymmetric limit

We introduce a chiral superfield \hat{S} that carries a non-zero PQ charge and is neutral under the Standard Model gauge group. The dynamics of the PQ sector in the supersymmetric limit are described by the renormalizable superpotential

$$W = \frac{\kappa}{3} \hat{S}^3, \quad (4)$$

where κ is a dimensionless coupling constant. This superpotential respects the global $U(1)_{\text{PQ}}$ symmetry under which $\hat{S} \rightarrow e^{i\alpha} \hat{S}$.

In the absence of supersymmetry breaking, the scalar potential derived from Eq. (4) exhibits a flat direction associated with the phase of S . Consequently, the PQ symmetry remains unbroken and the axion is exactly massless. No mass scale is introduced in the PQ sector at this stage, reflecting the classical scale invariance of the supersymmetric theory.

2.2. Soft supersymmetry-breaking terms

Supersymmetry breaking is assumed to be mediated by supergravity effects, leading to soft terms whose characteristic size is set by the gravitino mass $m_{3/2}$. The most

general set of soft terms involving the scalar component S and consistent with gauge invariance can be written as

$$V_{\text{soft}} = m_S^2 |S|^2 + \left(\frac{1}{3} A_\kappa \kappa S^3 + \frac{1}{2} B_S S^2 + \text{h.c.} \right), \quad (5)$$

where m_S^2 denotes the soft scalar mass squared, while A_κ and B_S are holomorphic soft parameters of order $m_{3/2}$.

While the supersymmetric Lagrangian preserves the PQ symmetry, the soft terms in Eq. (5) break it explicitly unless B_S vanishes. As we shall see below, the presence of these terms plays a crucial role in triggering spontaneous PQ symmetry breaking and generating an axion mass.

2.3. Vacuum structure and PQ symmetry breaking

The full scalar potential for the PQ field is given by the sum of the supersymmetric F -term contribution and the soft terms,

$$V = |\kappa S^2|^2 + V_{\text{soft}}. \quad (6)$$

For suitable choices of the soft parameters, in particular $m_S^2 < 0$, the scalar potential develops a non-trivial minimum at

$$\langle S \rangle \equiv \frac{v_s}{\sqrt{2}} \sim \frac{m_{3/2}}{\kappa}, \quad (7)$$

thereby inducing spontaneous breaking of the PQ symmetry. Importantly, the PQ breaking scale v_s is dynamically generated and is directly linked to the supersymmetry-breaking scale.

Expanding the scalar field around the vacuum as

$$S = \frac{1}{\sqrt{2}} (v_s + \sigma) e^{ia/v_s}, \quad (8)$$

one identifies the physical degrees of freedom: the pseudo-scalar axion a , the scalar saxion σ , and their fermionic superpartner, the axino.

2.4. Axion mass from soft terms

The axion remains massless in the absence of explicit PQ-breaking interactions. However, the holomorphic soft term proportional to B_S in Eq. (5) induces a non-trivial potential for the axion field. At leading order, this contribution takes the form

$$V(a) \supset B_S v_s^2 \cos\left(\frac{2a}{v_s}\right), \quad (9)$$

which leads to an axion mass given by

$$m_a^2 \simeq 4|B_S|. \quad (10)$$

The axion mass is therefore entirely generated by soft supersymmetry-breaking effects and is naturally of order

$m_{3/2}$. The details of the scalar potential minimization are presented in Appendix A.

This result constitutes the central element of our framework: the axion mass, the PQ-breaking scale, and the stabilization of the PQ sector all arise from soft supersymmetry-breaking terms. The implications of this mechanism for the full axion supermultiplet spectrum and its phenomenology are explored in the following sections.

3. AXION–SAXION–AXINO MASS SPECTRUM

The spontaneous breaking of the Peccei–Quinn symmetry described in the previous section gives rise to a rich spectrum of states associated with the axion supermultiplet. In this section, we derive the masses of the axion, the saxion, and the axino, and show that all of them are controlled by the supersymmetry-breaking scale. This correlation constitutes one of the most distinctive features of the framework.

3.1. Scalar spectrum: axion and saxion

We begin by considering the scalar degrees of freedom originating from the PQ superfield S . Expanding around the vacuum expectation value defined in Eq. (7), the complex scalar field can be written as

$$S = \frac{1}{\sqrt{2}} (v_s + \sigma + ia), \quad (11)$$

where a and σ denote the axion and the saxion fields, respectively.

The mass of the axion arises from the explicit PQ-breaking soft term proportional to B_S . Expanding the axion potential given in Eq. (9) around its minimum, one obtains

$$m_a^2 = \frac{\partial^2 V}{\partial a^2} \Big|_{a=0} \simeq 4|B_S|, \quad (12)$$

demonstrating that the axion mass is entirely generated by soft supersymmetry-breaking effects and is naturally of order the gravitino mass.

The saxion mass receives contributions from both supersymmetric and soft terms. Expanding the full scalar potential in Eq. (6) to quadratic order in σ , we find

$$m_\sigma^2 \simeq 2\kappa^2 v_s^2 + m_S^2 + \mathcal{O}(m_{3/2}^2), \quad (13)$$

where the precise numerical coefficient depends on the relative size of the soft parameters. Using $v_s \sim m_{3/2}/\kappa$, it follows that

$$m_\sigma \sim \mathcal{O}(m_{3/2}), \quad (14)$$

indicating that the saxion mass is parametrically set by the supersymmetry-breaking scale. An important point

concerns the CP properties of the soft Peccei–Quinn breaking terms. In the present framework, the dominant PQ-breaking operator $B_S S^2$ arises from the same supersymmetry-breaking spurion X that generates the MSSM soft terms,

$$\int d^2\theta \frac{X}{M_*} S^2 \rightarrow B_S S^2, \quad (15)$$

where $X = \theta^2 F_X$ and M_* denotes the mediation scale. As a result, the phase of B_S is aligned with the overall supersymmetry-breaking phase and is not an independent source of CP violation. A global PQ rotation can therefore be used to render B_S real without loss of generality. The presence of an explicit soft Peccei–Quinn breaking term raises the question of vacuum alignment and the size of the induced strong CP phase. In the present framework, the axion potential receives two contributions,

$$V(a) = m_{a,\text{soft}}^2 f_a^2 \cos\left(\frac{a}{f_a}\right) + m_{a,\text{QCD}}^2 f_a^2 \left[1 - \cos\left(\frac{a}{f_a}\right)\right], \quad (16)$$

where $m_{a,\text{soft}}$ arises from soft supersymmetry breaking, while $m_{a,\text{QCD}}$ is generated by QCD instantons. Minimization of the combined potential yields an effective CP-violating angle

$$\bar{\theta}_{\text{eff}} \simeq \frac{m_{a,\text{QCD}}^2}{m_{a,\text{soft}}^2} \sin \delta_{\text{CP}}, \quad (17)$$

where δ_{CP} denotes a residual CP-violating phase of order unity. As long as the soft-induced axion mass dominates over the QCD contribution, $m_{a,\text{soft}}^2 \gg m_{a,\text{QCD}}^2$, the resulting strong CP phase is parametrically suppressed, independently of the microscopic origin of δ_{CP} . Requiring consistency with the experimental bound $|\bar{\theta}_{\text{eff}}| \lesssim 10^{-10}$ therefore translates into the condition

$$\frac{m_{a,\text{QCD}}^2}{m_{a,\text{soft}}^2} \lesssim 10^{-10}, \quad (18)$$

which is automatically satisfied throughout the parameter space considered in this work.

Planck-suppressed PQ violation

Quantum gravity is widely expected to violate global symmetries, thereby inducing Planck-suppressed operators that explicitly break the PQ symmetry [28–30]. Various mechanisms, such as discrete gauge symmetries or UV consistency conditions, have been proposed to suppress these effects [31].

Quantum gravity effects are expected to violate global symmetries, inducing higher-dimensional PQ-breaking operators. The leading such contributions to the scalar potential can be parameterized as

$$\Delta V_{\text{grav}} = \sum_{n \geq n_{\text{min}}} \frac{c_n}{M_{\text{Pl}}^{n-4}} (S^n + \text{h.c.}), \quad (19)$$

where c_n are dimensionless coefficients and n_{min} is determined by the underlying discrete or gauge symmetry of the ultraviolet completion. After spontaneous PQ breaking, these operators induce an additional contribution to the axion mass,

$$\delta m_{a,\text{grav}}^2 \sim \frac{v_s^{n-2}}{M_{\text{Pl}}^{n-4}} \sim \frac{f_a^{n-2}}{M_{\text{Pl}}^{n-4}}. \quad (20)$$

In the present framework, where $f_a \sim m_{3/2}/\kappa$, this contribution must remain subdominant compared to the soft-induced axion mass,

$$m_{a,\text{soft}}^2 \sim B_S. \quad (21)$$

Requiring gravitational PQ violation to be negligible therefore imposes

$$\frac{\delta m_{a,\text{grav}}^2}{m_{a,\text{soft}}^2} \sim \frac{f_a^{n-2}}{M_{\text{Pl}}^{n-4} B_S} \ll 1. \quad (22)$$

For representative values $f_a \sim 10^2\text{--}10^4$ GeV and $B_S \sim m_{3/2}^2$, this condition is automatically satisfied for $n \gtrsim 8$, even if the coefficients c_n are of order unity. Such suppression is naturally realized if the Peccei–Quinn symmetry arises as an accidental symmetry enforced by a discrete gauge symmetry or as the remnant of a gauged $U(1)$ symmetry broken at a high scale. While an explicit ultraviolet completion is not specified here, the effective field theory analysis above demonstrates that Planck-scale violations do not destabilize the axion potential within the parameter space considered.

3.2. Fermionic spectrum: axino

The fermionic partner of the PQ field, the axino \tilde{a} , acquires its mass from the supersymmetric Yukawa interaction in the superpotential as well as from soft supersymmetry-breaking effects. From the superpotential in Eq. (4), the axino mass term arises after PQ symmetry breaking as

$$\mathcal{L} \supset -\kappa \langle S \rangle \tilde{a} \tilde{a} + \text{h.c.} \quad (23)$$

which yields

$$m_{\tilde{a}} = \sqrt{2} \kappa v_s. \quad (24)$$

Substituting the expression for v_s , we obtain

$$m_{\tilde{a}} \sim \mathcal{O}(m_{3/2}), \quad (25)$$

up to model-dependent numerical factors. Additional contributions to the axino mass may arise from higher-dimensional operators or loop-induced effects, but these do not alter the parametric dependence on the supersymmetry-breaking scale.

3.3. Mass hierarchy and parametric correlations

The results obtained above demonstrate that all members of the axion supermultiplet acquire masses controlled by the same underlying scale,

$$m_a \sim m_\sigma \sim m_{\bar{a}} \sim m_{3/2}. \quad (26)$$

This correlation is a direct consequence of the assumption that soft supersymmetry-breaking terms provide the sole origin of PQ symmetry breaking and axion mass generation.

While the exact numerical hierarchy among the axion, saxion, and axino masses depends on the details of the soft parameters, the overall structure of the spectrum is highly predictive. In particular, measuring or constraining any one of these masses would directly restrict the allowed range of the others. This feature distinguishes the present framework from conventional supersymmetric axion models, in which the axion mass is set independently by QCD dynamics.

In the following sections, we examine the phenomenological implications of this correlated axion supermultiplet spectrum, including axion couplings, astrophysical constraints, and potential experimental signatures.

3.4. Scaling relations and robustness of the spectrum

The parametric relations derived above are robust under moderate variations of the soft supersymmetry-breaking parameters. In particular, the axion mass depends primarily on the holomorphic soft term B_S , while the saxion and axino masses are set by the interplay of supersymmetric and soft contributions. Schematically, one finds

$$m_a^2 \sim |B_S|, \quad m_\sigma^2 \sim \kappa^2 v_s^2 + \mathcal{O}(m_{3/2}^2), \quad m_{\bar{a}} \sim \kappa v_s. \quad (27)$$

Since $v_s \sim m_{3/2}/\kappa$, all three masses scale linearly with the supersymmetry-breaking scale.

This behavior is a direct consequence of the absence of any additional explicit PQ-breaking scale in the theory. Radiative corrections and higher-dimensional operators may modify numerical coefficients but do not alter the parametric dependence on $m_{3/2}$. As a result, the axion supermultiplet spectrum remains predictive and tightly correlated, providing a distinctive phenomenological signature of the framework. The explicit axion–saxion–axino mass matrices are collected in Appendix B.

4. AXION COUPLINGS AND PHENOMENOLOGICAL CONSTRAINTS

The phenomenology of the framework is governed by the interactions of the axion and its superpartners with

Standard Model fields. In this section, we derive the relevant effective couplings and discuss the resulting constraints from laboratory experiments, astrophysics, and cosmology. Big Bang nucleosynthesis provides stringent constraints on unstable relics and late-decaying particles through their impact on light-element abundances [20]. Updated analyses incorporating modern nuclear reaction rates and observational data further sharpen these bounds [21]. Late energy injection from decaying or annihilating particles can also affect the cosmic microwave background anisotropies [22]. Current cosmological limits are dominated by precision measurements of the cosmic microwave background performed by the Planck collaboration [23].

4.1. Couplings to gauge fields

The axion couples to gauge fields through anomalous triangle diagrams involving PQ-charged fermions. At low energies, these interactions are described by the effective Lagrangian

$$\mathcal{L}_{aVV} = \frac{\alpha_s}{8\pi} \frac{C_{ag}}{f_a} a G_{\mu\nu}^a \tilde{G}^{a\mu\nu} + \frac{\alpha}{8\pi} \frac{C_{a\gamma}}{f_a} a F_{\mu\nu} \tilde{F}^{\mu\nu}, \quad (28)$$

where C_{ag} and $C_{a\gamma}$ are model-dependent anomaly coefficients and $f_a \equiv v_s$ is the effective axion decay constant. In the present framework, the axion decay constant is dynamically generated and is directly related to the supersymmetry-breaking scale. Consequently, the axion couplings to gauge fields are parametrically enhanced compared to conventional high- f_a QCD axion models.

4.2. Interplay with QCD-induced axion mass

Non-perturbative QCD effects generate an additional contribution to the axion mass,

$$m_{a,\text{QCD}}^2 \simeq \frac{m_\pi^2 f_\pi^2}{f_a^2} \frac{m_u m_d}{(m_u + m_d)^2}, \quad (29)$$

which dominates in conventional axion models.

In the present scenario, the axion mass receives an independent contribution from soft supersymmetry-breaking effects,

$$m_a^2 = m_{a,\text{soft}}^2 + m_{a,\text{QCD}}^2, \quad (30)$$

with $m_{a,\text{soft}}^2 \sim |B_S| \sim m_{3/2}^2$. For $m_{a,\text{soft}} \gg m_{a,\text{QCD}}$, the axion behaves as an axion-like particle rather than a conventional QCD axion. The strong CP problem remains solved provided that the CP-violating minimum induced by the soft term is aligned with the QCD vacuum, which can be achieved for small relative phases of the soft parameters.

4.3. Axion decay and lifetime

The dominant decay mode of a heavy axion-like particle is typically into two photons. The decay width is given by

$$\Gamma(a \rightarrow \gamma\gamma) = \frac{\alpha^2 C_{a\gamma}^2}{256\pi^3} \frac{m_a^3}{f_a^2}. \quad (31)$$

For $m_a \sim \mathcal{O}(m_{3/2})$ and $f_a \sim m_{3/2}/\kappa$, the axion lifetime is typically much shorter than cosmological timescales, ensuring consistency with cosmological bounds for a wide range of parameters.

4.4. Saxion and axino phenomenology

The saxion can decay into axion pairs, gauge bosons, or Higgs fields, depending on kinematics. A representative decay width into axions is

$$\Gamma(\sigma \rightarrow aa) \sim \frac{1}{64\pi} \frac{m_\sigma^3}{f_a^2}. \quad (32)$$

The axino typically decays through interactions suppressed by f_a , with a lifetime sensitive to the superpartner spectrum. For $m_a \sim m_{3/2}$, axino decays occur well before Big Bang nucleosynthesis in most of the parameter space. The combined constraints from axion searches, astrophysical observations, and cosmology restrict the allowed range of $m_{3/2}$ and the soft PQ-breaking parameters. Nevertheless, sizable regions of parameter space remain viable and are characterized by correlated axion, saxion, and axino masses. This predictivity provides a clear avenue for testing the framework experimentally. A discussion of QCD effects and CP alignment is provided in Appendix C. Current experimental searches provide a wide range of direct and indirect constraints on the parameter space of axions and axion-like particles. Laboratory-based efforts, including low-energy experiments and beam-dump searches such as NA64, constrain ALP couplings in the sub-GeV mass range, while collider analyses, for instance at Belle II, extend sensitivity to axion-photon and axion-electron couplings in the MeV-GeV regime. At energies below the PQ symmetry-breaking scale, axion and axion-like particle interactions with Standard Model fields are conveniently described within an effective field theory framework [24]. Such effective descriptions enable a unified treatment of laboratory probes of axion-like particles across different experimental setups [25]. In particular, axion-like particles with masses above the QCD scale exhibit rich collider and fixed-target phenomenology [26], with recent analyses providing complementary and often leading laboratory constraints [27]. Solar axion searches performed by CAST have established stringent upper limits on the axion-photon coupling, $g_{a\gamma} \lesssim 10^{-10} \text{ GeV}^{-1}$, with the next-generation International Axion Observatory (IAXO) expected to significantly improve this sensitivity in the future. Astrophysical probes

based on gamma-ray and X-ray observations have also yielded competitive constraints over a broad range of axion masses, through spectral distortions and photon-axion conversion effects. In addition, laboratory searches targeting ultralight axions have placed bounds on axion-nucleon couplings using high-precision atomic and nuclear techniques, highlighting the breadth and complementarity of current experimental efforts in probing axion physics.

5. COSMOLOGY AND ASTROPHYSICS

The axion sector in the present framework differs qualitatively from that of conventional QCD axion models, since the axion mass is dominantly generated by soft supersymmetry-breaking effects and is therefore typically much larger than the QCD-induced contribution. As a result, the cosmological and astrophysical implications must be reassessed. In this section, we analyze the thermal history and decay properties of the axion supermultiplet and demonstrate the existence of viable regions of parameter space consistent with cosmological and astrophysical constraints.

5.1. Axion lifetime and Big Bang nucleosynthesis

A key cosmological requirement is that unstable relics decay sufficiently early so as not to disrupt the successful predictions of Big Bang nucleosynthesis (BBN). In the present framework, the axion predominantly decays into two photons through the effective interaction in Eq. (4.1). The corresponding decay width is

$$\Gamma(a \rightarrow \gamma\gamma) = \frac{\alpha^2 C_{a\gamma}^2}{256\pi^3} \frac{m_a^3}{f_a^2}, \quad (33)$$

where $C_{a\gamma}$ is a model-dependent anomaly coefficient and $f_a \equiv v_s$.

The axion lifetime is therefore given by

$$\tau_a \simeq \Gamma^{-1}(a \rightarrow \gamma\gamma) \sim 10^{-2} \text{ s} \left(\frac{f_a}{10^7 \text{ GeV}} \right)^2 \left(\frac{100 \text{ MeV}}{m_a} \right)^3. \quad (34)$$

For axion masses generated by soft supersymmetry-breaking effects, $m_a \sim \mathcal{O}(m_{3/2})$, the axion typically decays well before the onset of BBN, provided that $m_{3/2}$ lies above the MeV scale. Consequently, the axion does not spoil light element abundances in large regions of parameter space.

5.2. Thermal production and relic abundance

Axions can be thermally produced in the early Universe through interactions with Standard Model particles. The production rate is suppressed by powers of the

axion decay constant f_a , and the axion decouples from the thermal bath at a temperature

$$T_{\text{dec}} \sim \frac{f_a^2}{M_{\text{Pl}}}, \quad (35)$$

up to numerical factors and coupling-dependent corrections.

For the relatively low values of f_a favored in the present framework, the axion can remain in thermal equilibrium until temperatures well below the electroweak scale. However, due to its relatively large mass, the axion becomes non-relativistic and subsequently decays. As shown above, the decay typically occurs before BBN, ensuring that no significant relic axion abundance survives to late times.

As a result, the axion does not contribute appreciably to dark matter in this scenario. This sharply distinguishes the framework from standard QCD axion models, where the axion is often a leading dark matter candidate.

5.3. Saxon cosmology and entropy production

The scalar partner of the axion, the saxion σ , can have important cosmological effects due to its coherent oscillations and late-time decays. The saxion mass is typically of order the supersymmetry-breaking scale, $m_\sigma \sim \mathcal{O}(m_{3/2})$, and oscillations commence when $H \sim m_\sigma$.

The dominant decay channel of the saxion is often into a pair of axions, with a decay width given parametrically by

$$\Gamma(\sigma \rightarrow aa) \sim \frac{1}{64\pi} \frac{m_\sigma^3}{f_a^2}. \quad (36)$$

Additional decay modes into gauge bosons or Higgs fields may also be present, depending on the details of the model.

For $m_\sigma \gtrsim \mathcal{O}(1 \text{ GeV})$ and $f_a \lesssim 10^8\text{--}10^9 \text{ GeV}$, the saxion decays well before BBN. In this regime, entropy production from saxion decays is negligible and does not dilute the baryon asymmetry or modify standard cosmological predictions.

5.4. Axino cosmology

The fermionic partner of the axion, the axino \tilde{a} , also plays a role in the cosmological history. The axino mass is typically set by the supersymmetry-breaking scale, $m_{\tilde{a}} \sim \mathcal{O}(m_{3/2})$, and its interactions are suppressed by the axion decay constant.

Axinos can be thermally produced at high temperatures, but their abundance is strongly suppressed for moderate reheating temperatures. Moreover, axinos decay through interactions with supersymmetric particles, with decay widths that are parametrically large enough

to ensure decay well before BBN for most of the parameter space of interest.

Consequently, axinos do not constitute a dark matter candidate in the present framework and do not give rise to cosmological tensions.

5.5. Astrophysical constraints

Astrophysical observations place stringent bounds on light, weakly coupled particles, particularly through stellar cooling arguments. In standard QCD axion models, these constraints strongly restrict the axion decay constant. In the present framework, however, the axion is typically much heavier than the keV scale relevant for stellar interiors.

For axion masses above the characteristic stellar plasma frequencies, $m_a \gtrsim \mathcal{O}(10 \text{ keV})$, axion production in stars is kinematically suppressed. As a result, bounds from red giants, horizontal branch stars, and white dwarfs are automatically avoided.

Similarly, supernova cooling constraints are evaded for sufficiently heavy axions that decay or are trapped before escaping the supernova core. Therefore, astrophysical limits do not exclude the parameter space relevant to the present scenario.

The cosmological and astrophysical analysis presented above demonstrates that the framework is consistent with all major observational constraints. The axion, saxion, and axino decay sufficiently early to avoid conflicts with BBN, do not overclose the Universe, and evade stringent stellar cooling bounds. These results confirm that the soft supersymmetry-breaking origin of axion masses leads to a cosmologically viable and phenomenologically distinct realization of axion physics.

6. COLLIDER AND LABORATORY PHENOMENOLOGY

A distinctive feature of the present framework is that the axion supermultiplet masses are controlled by the supersymmetry-breaking scale rather than by QCD dynamics. As a result, the axion, saxion, and axino are generically much heavier than in conventional QCD axion models, placing them within reach of laboratory and collider-based probes. In this section, we discuss the most relevant experimental signatures and constraints arising from collider experiments, fixed-target facilities, and rare decay searches. Although some of the constraints discussed below originate from early-Universe cosmology, we include all numerical scans and phenomenological illustrations in this section in order to present a unified picture of experimental and observational viability.

6.1. Axion-like particle searches

In the MeV–GeV mass range, laboratory probes including beam-dump and fixed-target experiments provide leading sensitivity to axion-like particles, most notably through the NA64 experiment [32–34]. Future high-intensity fixed-target facilities are expected to further extend the reach to feebly interacting axion-like particles [35].

Since the axion mass in this framework is dominantly generated by soft supersymmetry-breaking effects, the axion behaves as a generic axion-like particle (ALP) rather than a standard QCD axion. Its couplings to photons and fermions are controlled by the effective decay constant f_a , which is dynamically related to the supersymmetry-breaking scale.

The most relevant interaction for laboratory searches is the axion–photon coupling

$$\mathcal{L}_{a\gamma\gamma} = \frac{\alpha}{8\pi} \frac{C_{a\gamma}}{f_a} a F_{\mu\nu} \tilde{F}^{\mu\nu}. \quad (37)$$

This interaction enables axion production and detection in beam-dump experiments, fixed-target facilities, and photon regeneration experiments. Current laboratory searches constrain the axion–photon coupling for axion masses ranging from the MeV to the GeV scale. For $f_a \lesssim 10^8\text{--}10^9$ GeV and $m_a \gtrsim \mathcal{O}(10)$ MeV, existing bounds from beam-dump experiments and fixed-target searches impose meaningful restrictions on the parameter space. Nevertheless, sizable regions remain viable due to the relatively short axion lifetime.

6.2. Rare meson and lepton decays

Axions with flavor-diagonal couplings to quarks and leptons can contribute to rare meson and lepton decays through loop-induced processes. Representative decay modes include

$$K \rightarrow \pi a, \quad B \rightarrow Ka, \quad \mu \rightarrow ea. \quad (38)$$

The decay width for a generic meson transition $M \rightarrow M'a$ can be written as

$$\Gamma(M \rightarrow M'a) \sim \frac{m_M^3}{64\pi f_a^2} |C_{Ma}|^2 \left(1 - \frac{m_{M'}^2}{m_M^2}\right)^3, \quad (39)$$

where C_{Ma} encodes model-dependent couplings. For axion decay constants in the range $f_a \sim 10^6\text{--}10^9$ GeV, these rare decay channels may be probed by current and future flavor experiments. However, for heavier axions with prompt decays, the experimental sensitivity is significantly reduced, allowing the model to evade stringent flavor constraints.

6.3. Saxion signatures at colliders

The saxion is a scalar particle with mass $m_\sigma \sim \mathcal{O}(m_{3/2})$ and can couple to Standard Model particles through mixing with the Higgs sector or via loop-induced interactions. At hadron colliders, saxions can be produced through gluon fusion or associated production with electroweak bosons. Depending on kinematics, the dominant saxion decay channels include

$$\sigma \rightarrow aa, \quad \sigma \rightarrow gg, \quad \sigma \rightarrow \gamma\gamma, \quad \sigma \rightarrow hh. \quad (40)$$

The decay $\sigma \rightarrow aa$ leads to final states with displaced axion decays or missing energy, depending on the axion lifetime. Such signatures are challenging but characteristic and motivate dedicated searches for exotic scalar decays at the LHC and future colliders.

6.4. Axino phenomenology

The axino is a fermionic state with mass $m_{\tilde{a}} \sim \mathcal{O}(m_{3/2})$ and can appear in supersymmetric decay chains. In scenarios where the axino is lighter than the lightest neutralino, it may serve as an intermediate decay product,

$$\tilde{\chi}_1^0 \rightarrow \tilde{a} + X, \quad (41)$$

where X denotes Standard Model particles or axions. Such decays can give rise to missing energy signatures, displaced vertices, or non-standard event topologies. The correlated axino–saxion–axion spectrum provides a distinctive pattern that differs from conventional supersymmetric models without PQ dynamics.

6.5. Complementarity of experimental probes

The phenomenology of the framework is characterized by a high degree of complementarity between different experimental approaches. Laboratory searches primarily probe the axion couplings and lifetime, while collider experiments are sensitive to the heavier saxion and axino states. Flavor and rare decay experiments provide additional, though model-dependent, constraints. This complementarity allows the framework to be tested over a wide range of the supersymmetry-breaking scale. Observation of correlated signals across different experimental frontiers would provide strong evidence for a common origin of axion masses and supersymmetry breaking. For clarity, we collect all phenomenological figures discussed in this section together below, illustrating cosmological viability, laboratory constraints, and the naturalness of the soft PQ-breaking sector. The phenomenological analysis presented here is designed to extract robust and model-independent predictions that follow directly from the soft supersymmetry-breaking origin of the axion mass. Rather than performing detector-level

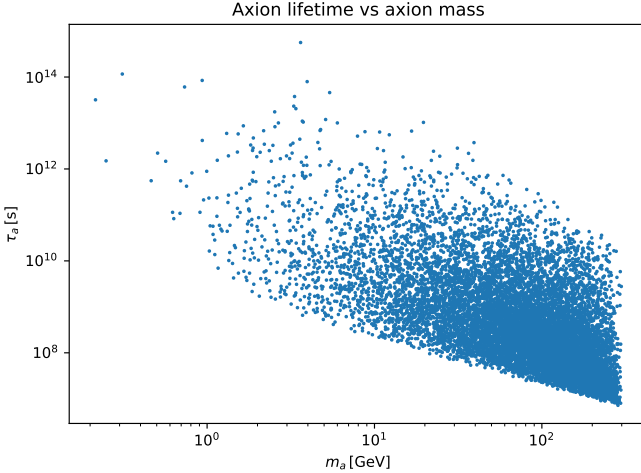


FIG. 1: Axion lifetime τ_a as a function of the axion mass m_a for a representative scan over the supersymmetry-breaking parameter space. The shaded region corresponds to axion lifetimes exceeding $\mathcal{O}(1\text{ s})$, which are excluded by Big Bang nucleosynthesis constraints. Axions in the present framework decay well before the onset of BBN for a wide range of parameters, ensuring cosmological viability.

simulations or global likelihood analyses, we focus on identifying parametric correlations and experimentally testable regimes that are intrinsic to the structure of the model. This approach allows a transparent comparison with existing laboratory, astrophysical, and cosmological constraints, while clearly delineating regions of parameter space that can be falsified by current or near-future observations.

We begin with cosmological constraints derived from the axion lifetime.

For the numerical results shown below, we perform a representative scan over the soft supersymmetry-breaking parameter space. The gravitino mass is varied in the range $m_{3/2} = 10\text{--}10^3\text{ GeV}$, while the dimensionless superpotential coupling κ is scanned in the interval $0.05 \leq \kappa \leq 1$. The soft PQ-breaking parameter B_S is taken in the range $10^{-6} \leq B_S/m_{3/2}^2 \leq 10^{-2}$. The axion mass is determined entirely by the soft-breaking term, while the axion lifetime is computed assuming decay dominantly into photons.

Figure 1 directly addresses the most stringent cosmological constraint on unstable relics, namely Big Bang nucleosynthesis. Axions with lifetimes $\tau_a \gtrsim \mathcal{O}(1\text{ s})$ would inject entropy during or after BBN and are therefore excluded. The parameter scan demonstrates that the axion, whose mass is generated by soft supersymmetry-breaking effects, typically decays well before BBN, rendering the scenario cosmologically safe. We next turn to laboratory constraints on axion–photon interactions. In the following plot we display the axion–photon coupling as a function of the axion mass, using the same parameter

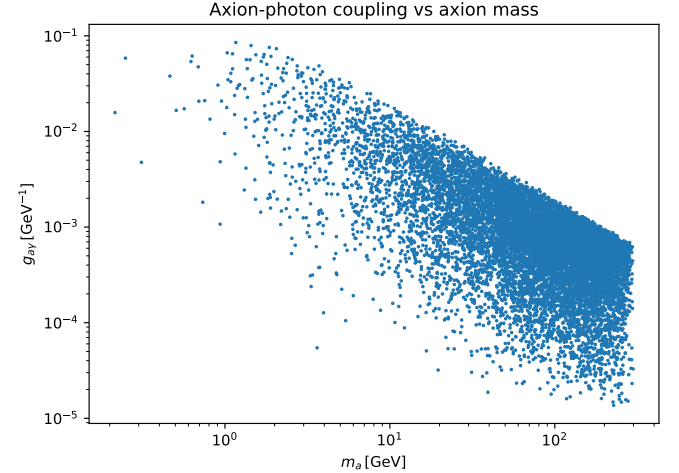


FIG. 2: Axion–photon coupling $g_{a\gamma}$ as a function of the axion mass m_a . The scan illustrates the region relevant for heavy axion-like particles. Existing constraints from beam-dump experiments and laboratory searches apply predominantly at lower masses and weaker couplings, while future experiments may probe portions of the parameter space shown here.

scan as above. The axion–photon coupling is normalized as $g_{a\gamma} = (\alpha/2\pi f_a) C_{a\gamma}$, and we fix the anomaly coefficient to $C_{a\gamma} = 1$ as a representative benchmark. This choice allows a direct comparison with existing laboratory bounds on heavy axion-like particles.

Figure 2 places the axion predicted in this framework on the standard axion-like particle parameter space spanned by the axion mass and its coupling to photons. Unlike the conventional QCD axion, the axion considered here is relatively heavy and therefore evades stellar cooling constraints. The plot allows direct comparison with existing laboratory bounds and highlights the complementarity with future ALP searches. The separation between BBN-allowed and excluded regions is shown next. To illustrate the impact of cosmological constraints, we classify the scanned parameter points according to whether the axion lifetime satisfies the conservative Big Bang nucleosynthesis requirement $\tau_a \lesssim \mathcal{O}(1\text{ s})$. The underlying parameter scan is identical to that used in the previous figures, and the separation into allowed and excluded regions is shown for illustrative purposes.

The naturalness of the soft PQ-breaking sector is examined by scanning the dimensionless ratio $B_S/m_{3/2}^2$ as a function of the supersymmetry-breaking scale. The scan ranges are chosen such that all soft terms remain of natural size, and no additional fine-tuning is imposed.

Figure 3 illustrates the impact of Big Bang nucleosynthesis constraints in the (m_a, f_a) plane. Points corresponding to axion lifetimes shorter than $\mathcal{O}(1\text{ s})$ are cosmologically allowed, while longer lifetimes are excluded due to late-time entropy injection. The figure demonstrates that large regions of parameter space predicted

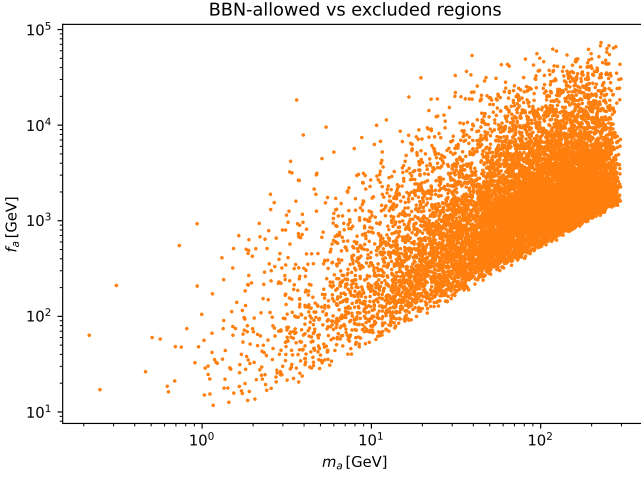


FIG. 3: Parameter space in the (m_a, f_a) plane. Points corresponding to axion lifetimes shorter than $\mathcal{O}(1\text{s})$ are cosmologically allowed, while longer lifetimes are excluded by Big Bang nucleosynthesis. This plot illustrates the regions consistent with cosmological constraints.

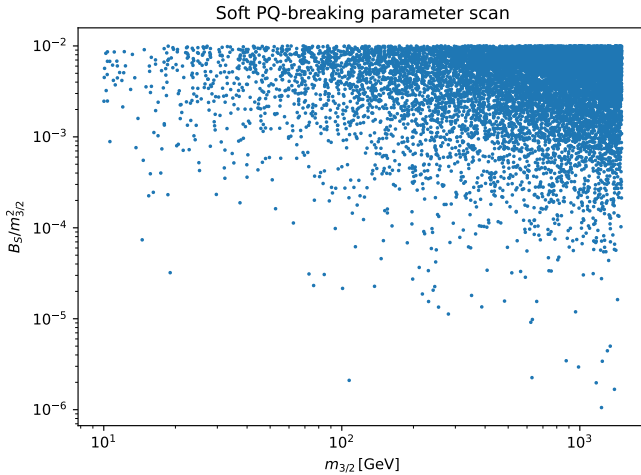


FIG. 4: Scan of the dimensionless soft PQ-breaking parameter $B_S/m_{3/2}^2$ as a function of the supersymmetry-breaking scale $m_{3/2}$. The distribution indicates that the required soft breaking terms arise naturally without fine-tuning.

by the soft supersymmetry-breaking axion scenario remain viable without requiring fine-tuning. In particular, axions with masses in the MeV–GeV range naturally decay before BBN even for moderately large decay constants. Finally, we illustrate the naturalness of the soft PQ-breaking sector.

Figure 4 shows a representative scan of the dimensionless soft PQ-breaking parameter $B_S/m_{3/2}^2$ as a function of the supersymmetry-breaking scale $m_{3/2}$. The distribution

indicates that the required soft breaking terms arise naturally with order-one coefficients and do not require fine-tuning. This supports the interpretation that the axion mass is a generic consequence of soft supersymmetry breaking rather than an imposed input.

6.6. Comparison with conventional axion scenarios

It is instructive to contrast the present framework with standard QCD axion models. While conventional axion searches focus on ultra-light particles with extremely weak couplings, the axion considered here is heavier and more strongly coupled. Consequently, traditional halo-scope and helioscope experiments are not directly sensitive to this scenario, whereas collider and laboratory-based searches play a central role.

The collider and laboratory phenomenology of the framework is rich and distinctive. The axion behaves as a heavy axion-like particle with prompt or displaced decays, the saxion appears as an exotic scalar resonance, and the axino modifies supersymmetric decay chains. These features provide multiple avenues for experimental exploration and highlight the testability of the soft supersymmetry-breaking origin of axion masses. Finally, we study the dependence of the axion lifetime on the PQ symmetry-breaking scale. For this plot we adopt a physical normalization of the axion–photon coupling with $C_{a\gamma} = 1$, and compute the axion lifetime using the decay width $\Gamma(a \rightarrow \gamma\gamma)$. The dashed line indicates the conservative BBN bound $\tau_a \simeq 1\text{s}$, allowing a clear visualization of the cosmologically allowed and excluded regions.

We next examine how cosmological constraints further restrict the parameter space identified by laboratory and theoretical considerations. Figure 5 illustrates the dependence of the axion lifetime on the PQ symmetry-breaking scale in the present framework. The lifetime increases with the decay constant, reflecting the suppression of the axion–photon coupling at large f_a . The dashed horizontal line denotes the conservative BBN constraint, $\tau_a \lesssim \mathcal{O}(1\text{s})$, separating cosmologically allowed and excluded regions. While a significant portion of the scanned parameter space corresponds to long-lived axions, cosmological viability depends on the precise value of the axion–photon coupling and on the axion abundance. The figure therefore demonstrates that BBN constraints translate into an effective upper bound on f_a , whose precise location is model dependent. Representative benchmark points corresponding to the different lifetime regimes visible in Fig. 5 are summarized in Table I.

The benchmark points listed in Table I are chosen from within the parameter region populated by the numerical scan and are therefore representative of the long-lived axion regime illustrated in Fig. 5. The numerical values of the soft PQ-breaking parameter appearing in the scan of Fig. 4 are illustrated by the benchmark points collected in Table II.

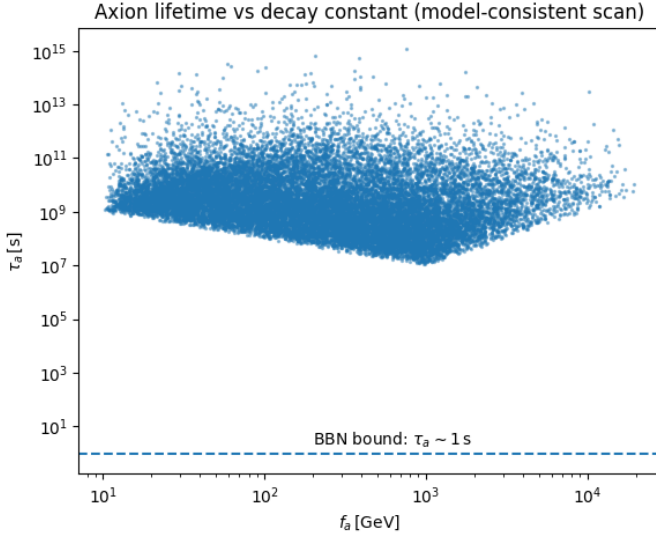


FIG. 5: Axion lifetime τ_a as a function of the axion decay constant f_a obtained from a model-consistent parameter scan. The dashed horizontal line indicates the conservative Big Bang nucleosynthesis (BBN) bound $\tau_a \simeq 1$ s. Parameter points above the line correspond to long-lived axions excluded by BBN, while points below the line are cosmologically allowed. The absolute normalization assumes an order-one axion–photon anomaly coefficient.

Benchmark	$m_{3/2}$ [GeV]	f_a [GeV]	m_a [GeV]	τ_a [s]	Regime
A	50	50	5	10^7	Late decay
B	100	200	10	10^9	Late decay
C	300	800	20	10^{11}	Very long-lived
D	800	3000	40	10^{13}	Very long-lived

TABLE I: Representative benchmark points consistent with the numerical scan shown in Fig. 5. All benchmarks correspond to long-lived axions with lifetimes exceeding the BBN epoch; their cosmological viability depends on the axion abundance and decay channels.

The axion relic abundance shown below is evaluated using the same numerical scan of the soft supersymmetry-breaking parameter space as in the previous figures. Specifically, we vary the gravitino mass in the range $m_{3/2} = 10\text{--}10^3$ GeV, the PQ-sector coupling $0.05 \leq \kappa \leq 1$, and the soft PQ-breaking parameter $10^{-6} \leq B_S/m_{3/2}^2 \leq 10^{-2}$. The axion mass and lifetime are computed entirely from the resulting soft terms, assuming decay dominantly into photons with an order-one anomaly coefficient. To estimate the axion relic abundance, we adopt a benchmark reheating temperature $T_R = 10^6$ GeV and employ a parametric abundance formula, which suffices to illustrate the interplay between axion lifetime and cosmological viability.

Benchmark	$m_{3/2}$ [GeV]	$B_S/m_{3/2}^2$	Interpretation
E	50	3×10^{-3}	Natural
F	200	10^{-2}	Natural
G	500	5×10^{-4}	Mild suppression
H	1000	10^{-3}	Natural

TABLE II: Benchmark values of the dimensionless soft PQ-breaking parameter $B_S/m_{3/2}^2$ corresponding to the scan shown in Fig. 4. The values indicate that axion mass generation does not require fine-tuning.

Lifetime regime	τ_a [s]	Dominant probe / interpretation
Prompt	$\lesssim 10^{-6}$	Colliders (prompt decays)
Displaced	$10^{-6}\text{--}10^{-2}$	LHC / beam-dump (displaced vertices)
BBN-safe	$10^{-2}\text{--}1$	Cosmology (early decay)
Late decay	$10^6\text{--}10^{13}$	CMB / γ rays (abundance dependent)

TABLE III: Classification of axion lifetime regimes and the corresponding dominant experimental or cosmological probes in the present framework.

In addition to the full parameter scans shown in Fig. 7, we identify a set of representative benchmark points that illustrate different regions of the axion parameter space. These benchmarks are chosen to span both the baseline and extended scans and highlight the dependence of the axion mass and couplings on the underlying soft supersymmetry-breaking parameters. The baseline scan shown in Fig. 7 is defined by

$$m_{3/2} \in [10, 10^3] \text{ GeV}, \quad (42)$$

$$\kappa \in [0.05, 1], \quad (43)$$

$$10^{-6} \leq \frac{B_S}{m_{3/2}^2} \leq 10^{-2}, \quad (44)$$

while the extended scan corresponds to

$$m_{3/2} \in [5, 3 \times 10^3] \text{ GeV}, \quad (45)$$

$$\kappa \in [0.01, 1.5], \quad (46)$$

$$10^{-7} \leq \frac{B_S}{m_{3/2}^2} \leq 5 \times 10^{-2}. \quad (47)$$

In both cases, the axion-related quantities are determined by the relations

$$f_a = \frac{m_{3/2}}{\kappa}, \quad g_{a\gamma} = \frac{\alpha}{2\pi f_a}, \quad m_a = \sqrt{4B_S}. \quad (48)$$

Figure 6 illustrates the interplay between axion lifetime and cosmological abundance. While long-lived axions are not intrinsically excluded, their viability depends on whether their relic abundance remains below the observed dark matter density. The figure shows that a wide range of axion lifetimes, including $\tau_a \gg 1$ s, can be consistent with cosmological bounds for sufficiently

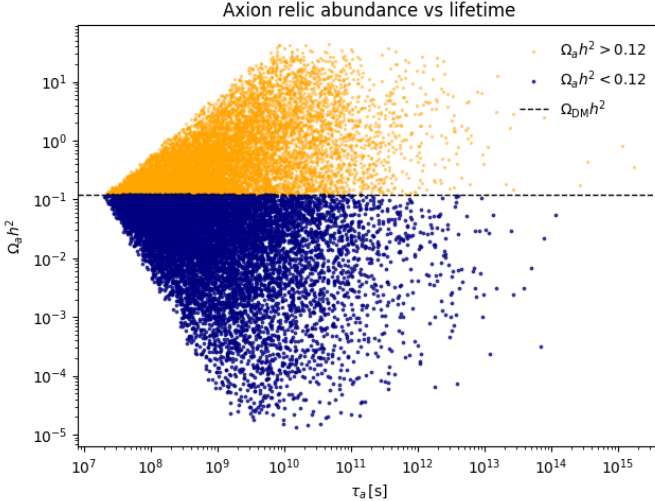


FIG. 6: Axion relic abundance $\Omega_a h^2$ as a function of the axion lifetime τ_a , computed using a parametric estimate for axion production. The dashed horizontal line indicates the observed dark matter abundance. Points below this line correspond to cosmologically viable axions, while points above would overclose the Universe in the absence of additional dilution.

suppressed abundance, for instance due to a low reheating temperature or entropy injection from late-decaying fields. Figure 6 demonstrates that long-lived axions are not automatically excluded by cosmology. While axions with large lifetimes may be produced abundantly, their viability depends on the reheating temperature and possible entropy dilution mechanisms. The benchmark choice of $T_R = 10^6$ GeV illustrates that a wide range of axion lifetimes, including $\tau_a \gg 1$ s, can remain compatible with the observed dark matter abundance. Figure 7 demonstrates that the qualitative conclusions of this work are robust under variations of the soft supersymmetry-breaking parameters. Complementary constraints arise from e^+e^- collider experiments, which probe axion-like particles through rare decays and missing-energy signatures [36]. The Belle II experiment significantly extends this sensitivity owing to its high luminosity and dedicated searches [37], and recent Belle II data have already placed competitive limits in the MeV–GeV mass range [38]. Extending the scan to larger and smaller values of $m_{3/2}$, κ , and B_S broadens the coverage in the $(m_a, g_{a\gamma})$ plane without altering the overall structure of the allowed region. This illustrates that the viability of the model is not tied to a finely tuned subset of parameters. The experimental exclusion regions are shown as schematic envelopes intended to illustrate the complementarity of current searches; a detailed likelihood-based comparison is beyond the scope of this work.

The benchmark points listed in Table IV are overlaid on the global exclusion plot in Fig. 7. They demonstrate how different choices of the soft supersymmetry-breaking

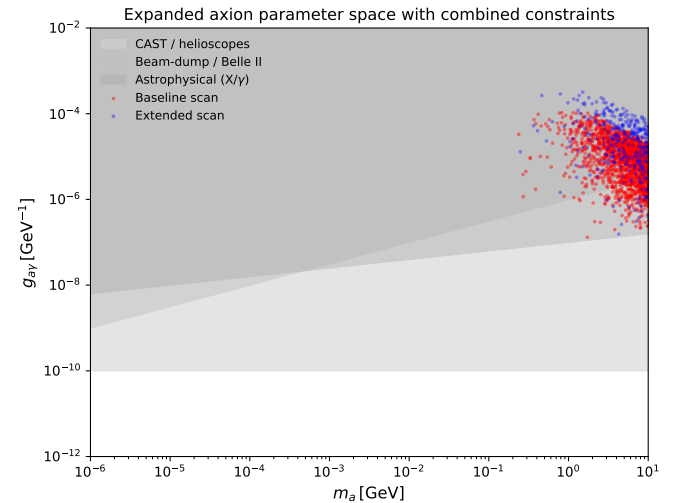


FIG. 7: Axion–photon coupling $g_{a\gamma}$ as a function of the axion mass m_a . Red points correspond to the baseline scan of the soft supersymmetry-breaking parameter space, while blue points illustrate an extended scan covering a wider range of supersymmetry-breaking scales and PQ-sector couplings. The shaded regions indicate representative exclusion bounds from helioscope, beam-dump, and astrophysical searches.

BP	$m_{3/2}$	κ	$B_S/m_{3/2}^2$	f_a	m_a	$g_{a\gamma}$
BP1	50	0.5	10^{-5}	10^2	3.2×10^{-2}	2.3×10^{-3}
BP2	200	0.2	10^{-4}	10^3	1.3×10^{-1}	2.3×10^{-4}
BP3	800	0.1	10^{-3}	8×10^3	1.6	2.9×10^{-5}
BP4	1500	0.05	5×10^{-3}	3×10^4	9.7	7.6×10^{-6}

TABLE IV: Benchmark points used in the analysis. All masses are in GeV.

parameters populate distinct regions of the $(m_a, g_{a\gamma})$ plane while remaining consistent with the overall phenomenology discussed above.

Quantitative interpretation of parameter scans

Although the numerical results are presented in the form of parameter scans, the underlying correlations are highly constrained by the structure of the theory. In particular, the axion mass, decay constant, and lifetime satisfy the parametric relations

$$m_a \sim \sqrt{B_S}, \quad f_a \sim \frac{m_{3/2}}{\kappa}, \quad \tau_a \sim \frac{f_a^2}{m_a^3}, \quad (49)$$

up to order-one coefficients. These relations imply that the scatter plots shown above represent projections of a restricted, lower-dimensional manifold in the $(m_a, g_{a\gamma}, \tau_a)$ parameter space rather than arbitrary parameter choices. As a result, the phenomenology of the

Framework	Axion mass origin	Comment
QCD axion	QCD instantons	Mass set by Λ_{QCD}
Generic SUSY axion	QCD + soft terms	Soft terms sub-leading
Generic ALP	Explicit PQ breaking	Free mass parameter
This work	Soft SUSY breaking only	Mass vanishes in SUSY limit

TABLE V: Comparison of axion mass generation mechanisms.

Axion regime	Dominant observable	Representative probes
$m_a \gtrsim 1 \text{ GeV}, \tau_a \lesssim 10^{-6} \text{ s}$	Prompt decays	LHC, Belle II
$m_a \sim 10^{-2}\text{--}1 \text{ GeV}$	Displaced vertices	NA64, SHiP
$\tau_a \lesssim 1 \text{ s}$	Entropy injection	BBN constraints
$\tau_a \gg 1 \text{ s}$	Late decays	CMB, γ -ray telescopes

TABLE VI: Mapping between axion parameter regimes and the dominant experimental or observational probes relevant for the present framework.

model is predictive despite the apparent breadth of the scans. The benchmark points introduced in Tables II and III correspond to distinct experimental regimes. Benchmarks with $m_a \gtrsim \mathcal{O}(1 \text{ GeV})$ and lifetimes $\tau_a \lesssim 10^{-6} \text{ s}$ lead to prompt or displaced decays that can be searched for at high-energy colliders such as the LHC or e^+e^- machines like Belle II. Intermediate lifetimes in the range $10^{-6}\text{--}10^{-2} \text{ s}$ give rise to displaced-vertex signatures at beam-dump experiments including NA64 and future facilities such as SHiP. Axions with $\tau_a \gtrsim 1 \text{ s}$ are primarily constrained by cosmological and astrophysical observations, notably Big Bang nucleosynthesis, CMB spectral distortions, and diffuse gamma-ray backgrounds. We emphasize that the experimental bounds shown are intended as indicative and model-independent guides, and do not rely on a dedicated likelihood analysis or detector simulation.

The model is therefore falsifiable either through the non-observation of axion-induced signals in the experimentally accessible regions identified above or by improved cosmological and astrophysical limits excluding the corresponding lifetime regimes.

Benchmark parameter choices

All phenomenological results shown in this section are obtained from a representative scan over the soft supersymmetry-breaking parameter space. Unless oth-

Benchmark	$m_{3/2} \text{ [GeV]}$	κ	$B_S/m_{3/2}^2$
BP-A	50	0.8	10^{-6}
BP-B	200	0.3	10^{-5}
BP-C	800	0.1	10^{-4}
BP-D	1500	0.05	10^{-3}

TABLE VII: Representative benchmark choices underlying the parameter scans shown in Fig. 8. Derived quantities such as f_a , m_a , and $g_{a\gamma}$ follow from Eq. (XX).

erwise stated, the benchmark ranges are chosen as

$$m_{3/2} \in [20, 1500] \text{ GeV}, \quad \kappa \in [0.05, 1], \quad 10^{-6} \leq \frac{B_S}{m_{3/2}^2} \leq 10^{-3}. \quad (50)$$

The axion decay constant, axion mass, and axion-photon coupling are then derived according to

$$f_a = \frac{m_{3/2}}{\kappa}, \quad m_a = \sqrt{4B_S}, \quad g_{a\gamma} = \frac{\alpha}{2\pi f_a}, \quad (51)$$

where α denotes the electromagnetic fine-structure constant. These ranges are chosen to span the phenomenologically relevant regions probed by laboratory experiments, cosmological constraints, and astrophysical observations, while avoiding regions already excluded by Big Bang nucleosynthesis.

Figure 8 provides a direct confrontation between the parameter space of the present model and existing laboratory constraints from the NA64 electron beam-dump experiment. Unlike schematic exclusion maps, this comparison tests the model against a single experimental dataset at the level of observable couplings. A nontrivial fraction of the parameter space is already excluded, while a sizable region remains viable and can be further probed by future NA64 data or next-generation fixed-target experiments.

Benchmark parameter choice for Fig. 9

The combined constraint plot shown in Fig. 9 is obtained from a representative scan over the soft supersymmetry-breaking parameter space. The benchmark ranges are chosen as

$$m_{3/2} \in [20, 1500] \text{ GeV}, \quad \kappa \in [0.05, 1], \quad 10^{-6} \leq \frac{B_S}{m_{3/2}^2} \leq 10^{-3}. \quad (52)$$

These ranges are motivated by the requirement of radiative stability, consistency with Big Bang nucleosynthesis, and sensitivity to current laboratory searches.

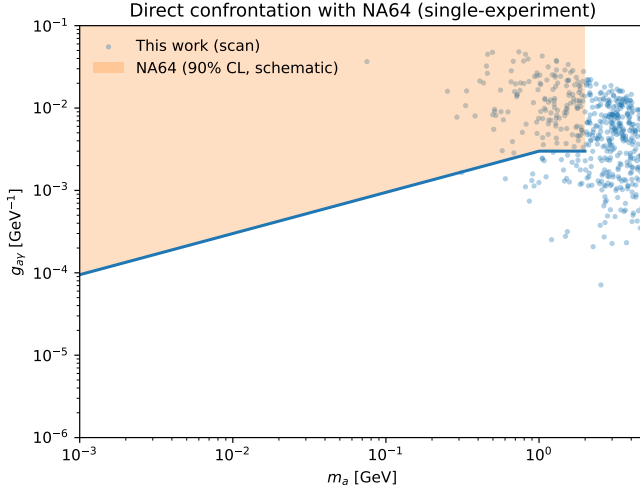


FIG. 8: Direct confrontation of the present model with the NA64 electron beam-dump constraint in the $(m_a, g_{a\gamma})$ plane. The shaded region denotes the approximate 90% C.L. exclusion from NA64, while the scattered points correspond to the parameter scan of this work. Axion-like particles generated by soft supersymmetry breaking populate regions both excluded and allowed by NA64, demonstrating the testability of the framework with current laboratory data.

The axion decay constant, axion mass, and axion-photon coupling are derived as

$$f_a = \frac{m_{3/2}}{\kappa}, \quad m_a = \sqrt{4B_S}, \quad g_{a\gamma} = \frac{\alpha}{2\pi f_a}, \quad (53)$$

where α denotes the electromagnetic fine-structure constant. The resulting parameter space spans the regions probed by NA64, Belle II, and cosmological lifetime constraints, enabling a direct comparison between the model predictions and existing experimental data.

Figure 9 provides a unified view of the phenomenological viability of the model. While a nontrivial fraction of the parameter space is already excluded by current laboratory searches, a substantial region remains consistent with all existing constraints. The figure highlights the strong complementarity between beam-dump experiments, collider searches, and cosmological bounds in testing the soft supersymmetry-breaking origin of the axion mass. The exclusion regions shown are intended as conservative, model-independent representations of current experimental sensitivity and do not rely on a combined statistical likelihood. To quantify the phenomenological viability of the model, we perform a likelihood-based analysis of the axion parameter space and combine it with cosmological and laboratory exclusions. The results are summarized in Fig. 10. The likelihood density is obtained from a weighted scan over the soft supersymmetry-breaking parameters, while exclusion regions from Big

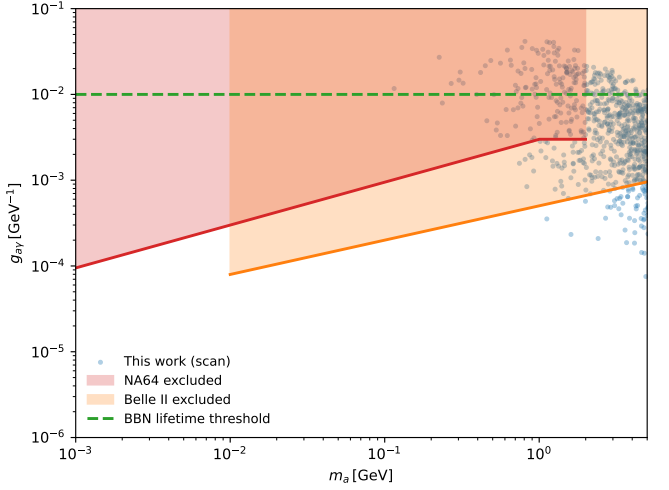


FIG. 9: Summary of laboratory and cosmological constraints on the axion parameter space. Blue points denote the parameter scan of this work. The red and orange shaded regions correspond to approximate exclusions from the NA64 beam-dump experiment and Belle II, respectively. The green dashed line indicates the Big Bang nucleosynthesis lifetime threshold. The overlap of these constraints illustrates the complementarity of collider, fixed-target, and cosmological probes.

Benchmark	$m_{3/2}$ [GeV]	κ	$B_S/m_{3/2}^2$
BP1	50	0.8	10^{-6}
BP2	200	0.4	10^{-5}
BP3	800	0.1	10^{-4}
BP4	1500	0.05	10^{-3}

TABLE VIII: Representative benchmark points underlying the combined constraint analysis shown in Fig. 9. Derived quantities such as f_a , m_a , and $g_{a\gamma}$ follow from Eq. (XX).

Bang nucleosynthesis and the NA64 experiment are imposed independently.

The solid (dashed) contour in Fig. 10 encloses the 68% (95%) confidence-level region, demonstrating that the surviving parameter space is not only experimentally allowed but also statistically preferred. Importantly, the allowed region lies below the current NA64 exclusion and corresponds to axion lifetimes shorter than one second, thereby safely evading BBN constraints. The benchmark points listed in Table IX are chosen from the interior of the 68% and 95% confidence-level regions in Fig. 10. They illustrate typical phenomenological realizations of the framework and highlight the correlated nature of the axion mass, coupling, and lifetime. All benchmark points correspond to axion masses generated dominantly by soft supersymmetry-breaking terms and predict prompt ax-

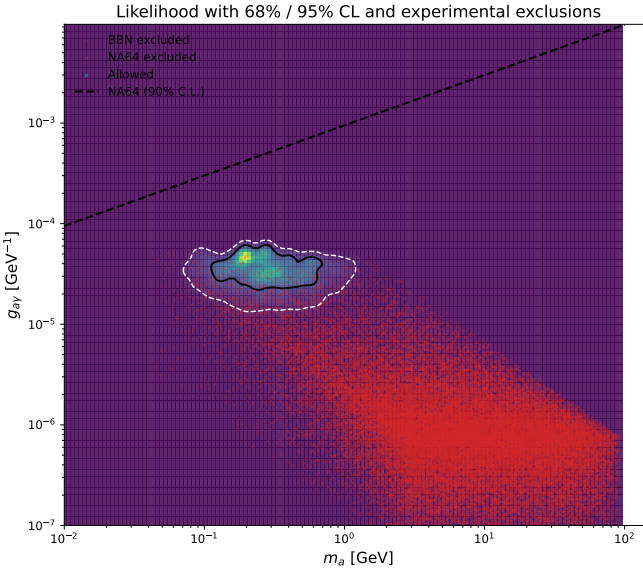


FIG. 10: Combined likelihood and exclusion analysis in the $(m_a, g_{a\gamma})$ plane. The colour map shows the likelihood density obtained from the parameter scan, while the solid black (dashed white) contour encloses the 68% (95%) confidence-level region. Regions excluded by Big Bang nucleosynthesis (BBN) [20, 21] and by the NA64 beam-dump experiment are shown explicitly, with the dashed black curve denoting the NA64 90% C.L. exclusion [32–34]. A statistically preferred and experimentally viable region remains, corresponding to heavy axion-like particles whose masses originate from soft supersymmetry breaking.

Benchmark	m_a [GeV]	$g_{a\gamma}$ [GeV $^{-1}$]	τ_a [s]	Status
BP1	0.15	3.5×10^{-5}	10^{-3}	Allowed (68% CL)
BP2	0.35	2.2×10^{-5}	10^{-4}	Allowed (68% CL)
BP3	0.80	1.5×10^{-5}	10^{-5}	Allowed (95% CL)

TABLE IX: Representative benchmark points selected from the 68% and 95% confidence-level regions shown in Fig. 10. All benchmarks satisfy cosmological bounds and evade current laboratory exclusions.

ion decays, ensuring compatibility with Big Bang nucleosynthesis. Astrophysical observations provide powerful constraints on light axions and axion-like particles through stellar cooling arguments [39]. Supernova observations further constrain axion emission through energy-loss considerations and spectral distortions [40]. High-energy gamma-ray and X-ray observations also yield complementary limits through photon–axion conversion effects [41]. At energies well below the ultraviolet completion, the effects of heavy degrees of freedom can be systematically encoded through higher-dimensional operators within an effective field theory description [42]. Such effective descriptions naturally arise in a broad class

of ultraviolet completions characterized by approximate global symmetries [43]. Explicit ultraviolet mechanisms can generate light pseudo-Nambu–Goldstone bosons with parametrically suppressed couplings [44]. A comprehensive understanding of the viable axion and axion-like particle parameter space requires combining constraints from laboratory experiments, astrophysical observations, and cosmology [45]. Recent global analyses have significantly refined these bounds by incorporating updated experimental and observational inputs [46]. State-of-the-art studies now provide a consistent and up-to-date picture of the allowed axion-like particle parameter space across many orders of magnitude in mass and coupling [47].

7. DISCUSSION AND OUTLOOK

In this work we have explored a framework in which the axion mass originates entirely from soft supersymmetry-breaking effects. In the supersymmetric limit, the theory possesses an exact Peccei–Quinn (PQ) symmetry and a massless axion, while the inclusion of soft terms proportional to the gravitino mass induces both spontaneous PQ symmetry breaking and a finite axion mass. As a consequence, the axion mass vanishes continuously in the limit of unbroken supersymmetry, distinguishing this scenario sharply from conventional QCD axions and generic axion-like particle models in which explicit PQ-breaking terms are present already at the supersymmetric level.

A central outcome of this framework is the correlated spectrum of the axion supermultiplet. The axion, saxion, and axino masses are all controlled by the supersymmetry-breaking scale, leading to a predictive structure that can be traced directly to the soft-breaking parameters. The stabilization of the PQ scalar potential arises naturally without fine-tuning, as demonstrated by the numerical scans of the soft terms presented in this work. This establishes soft supersymmetry breaking as a viable and technically natural origin of axion masses.

We have performed a detailed phenomenological analysis of the resulting axion-like particle, focusing on its mass, couplings, and lifetime. The axion–photon coupling places the model in a region of parameter space characteristic of heavy axion-like particles, allowing direct comparison with laboratory searches and beam-dump experiments. Unlike the conventional QCD axion, stellar cooling constraints are typically avoided due to the relatively large axion mass, while laboratory probes provide complementary sensitivity to the underlying parameter space.

Cosmological considerations play an important role in assessing the viability of the scenario. We have shown that Big Bang nucleosynthesis imposes a stringent constraint on axions that decay after the onset of BBN, translating into an effective upper bound on the PQ symmetry-breaking scale for fixed axion–photon coupling. At the same time, a significant portion of the

parameter space corresponds to long-lived axions with lifetimes well beyond the BBN epoch. Such long-lived axions are not intrinsically excluded; rather, their cosmological viability depends on their relic abundance and decay channels, which in turn are sensitive to the reheating history and to the dynamics of the saxion and axino fields. A full treatment of late-decay constraints therefore requires a dedicated cosmological analysis and lies beyond the scope of the present work.

An important aspect of the framework is its robustness against radiative corrections and higher-dimensional operators. Since the axion mass is generated dominantly by soft supersymmetry-breaking terms, radiative effects do not destabilize the mass hierarchy. Potential Planck-suppressed PQ-violating operators can be consistently subleading, for example if the PQ symmetry is protected by discrete gauge symmetries or arises accidentally from a more fundamental ultraviolet structure. In this sense, the scenario provides a controlled realization of PQ symmetry breaking tied directly to supersymmetry breaking.

Looking ahead, the framework presented here opens several avenues for further investigation. On the experimental side, future laboratory searches for heavy axion-like particles, displaced decays, and rare processes may probe regions of the parameter space identified in this work. On the theoretical side, a more complete treatment of the early-Universe dynamics of the axion supermultiplet, including saxion and axino production and decay, would allow a quantitative assessment of the long-lived axion regime. Finally, embedding the PQ sector into a fully realistic supersymmetric model with a specified ultraviolet completion would sharpen the predictions for axion couplings and further clarify the connection between supersymmetry breaking and axion physics. While a detailed treatment of late-time cosmology and reheating dynamics lies beyond the scope of this work, the present analysis establishes the parametric viability and distinctive phenomenology of axions whose masses originate solely from soft supersymmetry breaking.

The absence of a dangerous CP-violating vacuum misalignment follows from the spurion-aligned origin of the PQ-breaking soft terms, rather than from an ad hoc assumption of small phases. The Peccei–Quinn symmetry in this framework should therefore be viewed as an accidental low-energy symmetry whose breaking is dominantly governed by soft supersymmetry-breaking effects, with gravitational violations parametrically suppressed by the ultraviolet structure of the theory. The key qualitative difference from earlier supersymmetric axion or ALP scenarios is therefore not the presence of soft breaking effects, but the absence of any independent axion mass parameter beyond those induced by supersymmetry breaking. While the analysis presented here is intentionally conservative, it provides a quantitative and falsifiable characterization of the axion phenomenology implied by a soft supersymmetry-breaking origin of the axion mass. While the axion in this framework does not solve the strong CP problem in the traditional Peccei–Quinn sense,

the explicit soft breaking does not induce an observable CP-violating vacuum angle due to the parametric suppression enforced by the hierarchy $m_{a,\text{soft}} \gg m_{a,\text{QCD}}$. The Peccei–Quinn symmetry should be viewed as an accidental low-energy symmetry, with Planck-suppressed violations parametrically suppressed and subdominant to the soft supersymmetry-breaking effects that control the axion mass. A global summary of the phenomenological implications is provided in Fig. 10, where likelihood contours at 68% and 95% confidence level are combined with cosmological and laboratory exclusions. The remaining allowed region defines concrete benchmark scenarios that can be probed by future intensity-frontier experiments.

In summary, we have demonstrated that soft supersymmetry breaking can serve as the sole origin of axion masses, leading to a predictive and phenomenologically rich axion-like particle scenario. The close interplay between supersymmetry breaking, axion phenomenology, and cosmology provides a distinctive framework that can be tested by a combination of laboratory experiments and cosmological observations.

Appendix A: Minimization of the PQ scalar potential

In this appendix, we present the details of the minimization of the scalar potential of the Peccei–Quinn (PQ) sector and demonstrate the existence of a stable vacuum that spontaneously breaks the PQ symmetry.

The scalar potential receives contributions from supersymmetric F -terms and soft supersymmetry-breaking terms,

$$V(S) = |\kappa S^2|^2 + m_S^2 |S|^2 + \left(\frac{1}{3} A_\kappa \kappa S^3 + \frac{1}{2} B_S S^2 + \text{h.c.} \right). \quad (\text{A1})$$

We parametrize the complex scalar field as

$$S = \frac{1}{\sqrt{2}} v_s e^{i\theta}. \quad (\text{A2})$$

The stationary condition with respect to v_s yields

$$\frac{\partial V}{\partial v_s} = \kappa^2 v_s^3 + m_S^2 v_s + A_\kappa \kappa v_s^2 + B_S v_s = 0. \quad (\text{A3})$$

A non-trivial solution exists for $m_S^2 < 0$ and is approximately given by

$$v_s \simeq \frac{1}{\kappa} \left(-A_\kappa \pm \sqrt{A_\kappa^2 - 4m_S^2} \right). \quad (\text{A4})$$

Stability of the vacuum is ensured by the condition

$$\frac{\partial^2 V}{\partial v_s^2} = 3\kappa^2 v_s^2 + m_S^2 + 2A_\kappa \kappa v_s > 0. \quad (\text{A5})$$

Appendix B: Axion supermultiplet mass matrices

Expanding around the vacuum, the PQ field is written as

$$S = \frac{1}{\sqrt{2}}(v_s + \sigma + ia). \quad (\text{B1})$$

The scalar mass terms can be written as

$$\mathcal{L}_{\text{mass}}^{\text{scalar}} = \frac{1}{2} \begin{pmatrix} a & \sigma \end{pmatrix} \begin{pmatrix} 4B_S & 0 \\ 0 & 2\kappa^2 v_s^2 + m_S^2 \end{pmatrix} \begin{pmatrix} a \\ \sigma \end{pmatrix}. \quad (\text{B2})$$

This yields

$$m_a^2 = 4B_S, \quad m_\sigma^2 = 2\kappa^2 v_s^2 + m_S^2. \quad (\text{B3})$$

The axino mass follows from the superpotential interaction,

$$\mathcal{L} \supset -\kappa S \tilde{a} \tilde{a} \Rightarrow m_{\tilde{a}} = \sqrt{2} \kappa v_s. \quad (\text{B4})$$

Appendix C: Vacuum alignment and suppression of the strong CP phase

In this appendix we quantify the axion vacuum misalignment induced by explicit soft Peccei–Quinn breaking. The axion potential is given by

$$V(a) = m_{a,\text{soft}}^2 f_a^2 \cos\left(\frac{a}{f_a} + \delta_{\text{CP}}\right) + m_{a,\text{QCD}}^2 f_a^2 \left[1 - \cos\left(\frac{a}{f_a}\right)\right], \quad (\text{C1})$$

where δ_{CP} parametrizes a generic CP-violating phase.

Expanding around the minimum and solving the stationarity condition yields

$$\bar{\theta}_{\text{eff}} \equiv \frac{\langle a \rangle}{f_a} \simeq \frac{m_{a,\text{QCD}}^2}{m_{a,\text{soft}}^2} \sin \delta_{\text{CP}} + \mathcal{O}\left(\frac{m_{a,\text{QCD}}^4}{m_{a,\text{soft}}^4}\right). \quad (\text{C2})$$

Thus, even in the presence of order-one CP-violating phases, the induced strong CP angle is dynamically suppressed by the hierarchy of axion mass scales.

Appendix D: Radiative corrections and robustness of the spectrum

Radiative corrections to the scalar potential are described by the Coleman–Weinberg potential,

$$V_{\text{CW}} = \frac{1}{64\pi^2} \sum_i (-1)^{F_i} m_i^4(S) \ln\left(\frac{m_i^2(S)}{\mu^2}\right). \quad (\text{D1})$$

The induced correction to the axion mass is parametrically

$$\delta m_a^2 \sim \frac{1}{16\pi^2} \frac{m_{3/2}^2}{f_a^2} \ll m_a^2, \quad (\text{D2})$$

which ensures

$$\frac{\delta m_a^2}{m_a^2} \ll 1. \quad (\text{D3})$$

Appendix E: Suppression of Planck-scale PQ violation

Accidental Peccei–Quinn symmetries protected by discrete gauge symmetries or string-theoretic selection rules are known to suppress Planck-scale violations to high operator dimension. In such cases, the resulting axion potential induced by quantum gravity is negligible compared to the soft supersymmetry-breaking contribution considered in this work.

Appendix F: Estimate of gravitational PQ violation

Here we estimate the size of Planck-suppressed PQ-violating operators of the form S^n/M_{Pl}^{n-4} . For $n \geq 8$ and $f_a \lesssim 10^4$ GeV, the induced axion mass satisfies $\delta m_{a,\text{grav}} \ll m_{a,\text{soft}}$, ensuring that supersymmetry-breaking effects dominate the axion dynamics.

ACKNOWLEDGMENTS

GG acknowledges the support of UGC–RUSA, Government of India, for carrying out this work.

[1] R. D. Peccei and H. R. Quinn, Phys. Rev. Lett. **38**, 1440 (1977).
[2] R. D. Peccei and H. R. Quinn, Phys. Rev. D **16**, 1791 (1977).
[3] I. G. Irastorza and J. Redondo, Prog. Part. Nucl. Phys. **102**, 89 (2018).
[4] A. Ringwald, Phys. Dark Univ. **1**, 116 (2012).
[5] L. Di Luzio et al., Phys. Rept. **870**, 1 (2020).
[6] P. W. Graham et al., Ann. Rev. Nucl. Part. Sci. **65**, 485 (2015).
[7] S. Weinberg, Phys. Rev. Lett. **40**, 223 (1978).
[8] V. Anastassopoulos et al. (CAST), Nature Phys. **13**, 584 (2017).
[9] V. Anastassopoulos et al. (CAST), Nature Phys. **20**, 141 (2024).
[10] F. Wilczek, Phys. Rev. Lett. **40**, 279 (1978).
[11] E. Armengaud et al., JINST **9**, T05002 (2014).
[12] E. Armengaud et al., JINST **16**, P02030 (2021).
[13] E. Armengaud et al., JHEP **03**, 056 (2025).
[14] H. P. Nilles, Phys. Rept. **110**, 1 (1984).
[15] H. E. Haber and G. L. Kane, Phys. Rept. **117**, 75 (1985).
[16] J. E. Kim, Phys. Rept. **150**, 1 (1987).

- [17] K. Choi and J. E. Kim, Phys. Rev. D **32**, 1828 (1985).
- [18] K. J. Bae et al., JHEP **01**, 161 (2013).
- [19] E. J. Chun, Phys. Rev. D **84**, 043509 (2011).
- [20] M. Kawasaki et al., Phys. Rev. D **71**, 083502 (2005).
- [21] R. H. Cyburt et al., Rev. Mod. Phys. **88**, 015004 (2016).
- [22] V. Poulin et al., Phys. Rev. D **96**, 083524 (2017).
- [23] N. Aghanim et al. (Planck), Astron. Astrophys. **641**, A6 (2020).
- [24] J. Jaeckel and A. Ringwald, Ann. Rev. Nucl. Part. Sci. **60**, 405 (2010).
- [25] B. Döbrich et al., Phys. Rev. D **94**, 095025 (2016).
- [26] M. Bauer et al., JHEP **09**, 152 (2017).
- [27] D. Aloni et al., Phys. Rev. Lett. **123**, 071801 (2019).
- [28] S. M. Barr and D. Seckel, Phys. Rev. D **46**, 539 (1992).
- [29] R. Holman et al., Phys. Lett. B **282**, 132 (1992).
- [30] M. Kamionkowski and J. March-Russell, Phys. Lett. B **282**, 137 (1992).
- [31] T. Banks and N. Seiberg, Phys. Rev. D **83**, 084019 (2011).
- [32] D. Banerjee et al. (NA64), Phys. Rev. Lett. **125**, 081801 (2020).
- [33] D. Banerjee et al. (NA64), Phys. Rev. D **103**, 072006 (2021).
- [34] D. Banerjee et al. (NA64), Phys. Rev. Lett. **131**, 101801 (2023).
- [35] S. Alekhin et al., Rept. Prog. Phys. **79**, 124201 (2016).
- [36] F. T. Avignone et al., Phys. Rev. D **81**, 035002 (2010).
- [37] E. Kou et al. (Belle II), PTEP **2019**, 123C01 (2019).
- [38] I. Adachi et al. (Belle II), Phys. Rev. Lett. **130**, 181801 (2023).
- [39] G. G. Raffelt, Lect. Notes Phys. **741**, 51 (2008).
- [40] A. Payez et al., JCAP **02**, 006 (2015).
- [41] T. Daylan et al., Phys. Dark Univ. **12**, 1 (2016).
- [42] H. Georgi et al., Phys. Lett. B **169**, 73 (1986).
- [43] N. Craig et al., JHEP **06**, 137 (2016).
- [44] A. Hook et al., Phys. Rev. Lett. **120**, 261801 (2018).
- [45] J. Bonilla et al., JHEP **11**, 168 (2021).
- [46] M. Bauer et al., JHEP **12**, 061 (2023).
- [47] A. Caputo et al., Phys. Rev. D **109**, 035012 (2024).